Possible Ascorbic Acid Enhanced Therapeutic Effect of Hemopoietic and Mesenchymal Stem Cells on Early Diabetic Retinopathy Rat Model: Comparative Histo-Biophysiological Study

Asmaa Ahmed El-Shafei[1], Maha Baligh Zickri[1,2], Sahar Mahmoud Mansour[3], Marwa Ibrahim Abd El-Aziz[3], Hossam El Din Said Kareem[4], Mai Abdelaziz Gouda[5] and Doaa Mabrouk Khaled[6]

Original Article

[1]Department of Medical Histology & Cell Biology, Faculty of Medicine, Cairo University, [2]Faculty of Oral and Dental Medicine, Future University, Egypt (FUE)

[3]Department of Histology, [4]Department of Vision Science, Research Institute of Ophthalmology, Cairo, Egypt

[5]Department of Medical Biochemistry & Molecular Biology, Faculty of Medicine, Cairo University and Badr University in Cairo, Egypt

[6]Department of Histology & Cytology, Faculty of Medicine, Helwan University, Egypt

ABSTRACT

Introduction and Objectives: Diabetic retinopathy is a serious ocular complication of diabetes and the leading cause of blindness and loss of vision in developed and developing countries. The present study aimed to investigate and compare the possible ascorbic acid (AA)-enhanced therapeutic effect of bone marrow hemopoietic stem cells (BMHSCs) to adipose mesenchymal stem cells (AMSCs) on streptozotocin (STZ)-induced early diabetic retinopathy (DR) in male albino rat model.
Methods and Results: 30 adult male albino rats were divided into: Donor group: 2 rats for BMHSCs and AMSCs isolation and culture. Group I (Control Group): 6 rats, Group II (DR Group): 8 rats, 50 mg of STZ were injected intraperitoneally (IP), Diabetes was confirmed 3 days after STZ injection by monitoring blood glucose levels. Group III (DR BMHSCs and AA-treated Group): 7 rats, 1x106 BMHSCs, were injected IP combined with oral administration of AA at a dose of 500 mg/Kg daily and Group IV (DR AMSCs and AA-treated Group): 7 rats, 1x106 AMSCs were injected combined with AA as in group III following confirmation of diabetes. Groups I, II, III and IV were sacrificed 8 weeks following confirmation of diabetes. Electroretinogram (ERG), serological, biochemical, histological, morphometric and statistical studies were performed. In group II, neurodegenerative changes were found in the retina that regressed in groups III more obviously than IV. ERG, blood glucose, MDA, SOD, TNFα and qPCR were confirmative.
Conclusions: AA enhanced regenerative effect of BMHSCs was more obvious, suggesting the possibility of its application as a therapeutic modality for DR.

Received: 02 July 2022, **Accepted:** 08 September 2022

Key Words: AA, AMSCs, BMHSCs, DR, RPE65.

Corresponding Author: Doaa Mabrouk Khaled, PhD, Department of Histology & Cytology, Faculty of Medicine, Helwan University, Egypt, **Tel.**: +20 11 4993 9631, **E-mail:** doaa.khaled@med.helwan.edu.eg

ISSN: 1110-0559, Vol. 46, No. 4

INTRODUCTION

Diabetic retinopathy (DR) is one of the most common complications of diabetes mellitus (DM) and a leading cause of visual impairment & blindness in diabetics. The currently available treatments are not effective for all patients, being indicated only in advanced stages of the disease, and have significant side effects[1]. Between 1990 and 2015, the prevalence of DR-related visual impairment and blindness increased, especially in low- & middle-income countries[2].

Long-term DM can lead to serious secondary pathologies such as diabetic retinopathy due to vascular damage caused by persistently elevated blood glucose level. In ophthalmology, anti-vascular endothelial growth factor (VEGF) agents have become one of the most effective therapeutic modalities. Their use, however, is contraindicated in some patients and is associated with adverse effects including endophthalmitis and retinal detachment after intra-vitreal injection[3]. Hyperbaric oxygen therapy may improve DR but serves as an adjunctive treatment for retinal ischemia and capillary hyperpermeability. In addition, due to its cytotoxic properties it may cause cataract[4].

Hyperglycemia is thought to impair the mobilization of hematopoietic stem cells (HSCs) and progenitor cells from the bone marrow (BM) through induction of stem

 DOI: 10.21608/ejh.2022.146693.1714

cell niche malfunction. New glucose-lowering therapies are specifically targeting to prevent or treat diabetic complications[5].

Stem cell therapy has provided a new approach to treat the underlying ischemia that causes microvascular complications in diabetes. The use of mesenchymal stem cells (MSCs) and tissue engineering are considered as possible alternatives to current therapies[6].

Recent studies commented on cytochrome P (CYP46a1) gene deficiency in the retina precipitating typical retinal changes similar to DR[7]. Another recent study investigated the association of gene expression, development and incidence of DR and identified retinal pigmented epithelium (RPE65) gene. Both genes may be crucial for management of DR in the near future[8].

Ascorbic acid (AA) is a potent antioxidant with many uses in the pharmaceutical and medical fields. It is well-established that in diabetics, reactive oxygen species (ROS) accumulate and negatively affect organ and tissue function. Ascorbic acid may restore antioxidant defenses and improve the delivery of therapeutic agent to the active site[9].

The present work aimed to investigate and compare the possible (AA)-enhanced therapeutic effect of BMHSCs to AMSCs on streptozotocin (STZ)-induced early diabetic retinopathy (DR) in male albino rat model.

MATERIALS AND METHODS

Drugs

Streptozotocin: was supplied by Sigma Company (St. Louis, Mo, USA) as 1g vial in a powder form to be dissolved in citrate buffer.

Ascorbic Acid (AA): was supplied by Development of Chemical Industries (Giza, Egypt) in a 1g Vitacid C effervescent tablet form to be dissolved in water.

Animals

This study was conducted on 30 adult male albino rats (3-6 months) with an average body weight of 200 grams. They were housed in a well-ventilated room and kept in hygienic stainless-steel cages with 12 hours light/dark cycles in Kasr Al-Ainy Animal House, Faculty of Medicine, Cairo University. Animal Ethics Committee of Cairo University approved all procedures with approval number: CU III F 10 21.

Experimental Design

The rats were divided randomly into the following groups:

Donor Group, 2 rats: one rat was used for BMHSCs and the other for AMSCs isolation, culture, phenotyping and labeling.

Group I (Control Group), 6 rats: were equally divided into the following subgroups:

- Subgroup IA, 2 rats: each rat was injected intraperitoneally (IP) with a single dose of 0.5 ml citrate buffer (Vehicle of STZ).
- Subgroup IB, 2 rats: each rat received a single IP injection of 0.5 ml citrate buffer and then 4 weeks following confirmation of diabetes in the corresponding experimental group, a single dose of 1ml of phosphate buffered saline (PBS) (the vehicle of SCs) was given IP combined with a daily oral AA (500 mg/Kg) dissolved in 0.5 ml water using a syringe without its needle for another 4 weeks.
- Subgroup IC, 2 rats: each rat received citrate buffer, PBS and AA as in subgroup IB.

Group II (DR Group), 8 rats: For induction of diabetes, each rat was injected with a single IP dose of STZ (50 mg/kg body weight)[10] dissolved in 0.5 ml citrate buffer. Diabetes was confirmed 3 days after STZ injection by monitoring blood glucose levels. If the animals' blood glucose level was >200 mg/dl, they were considered as diabetic[11]. Four weeks following confirmation of diabetes, one rat was sacrificed to establish the early DR by microscopic examination of H&E- stained retinal sections according to Rong *et al*[12].

Group III (DR, BMHSCs and AA-treated Group), 7 rats: Induction & confirmation of diabetes and DR were done as in group II, then 4 weeks following confirmation, a single IP dose of $1x10^6$ cultured and Feridex labeled BMHSCs, suspended in 1ml PBS, was injected[13]. Combined daily oral administration of 500 mg/Kg of AA[14] dissolved in 0.5 ml of water was given for each rat for another 4 weeks using a syringe without its needle.

Group IV (DR, AMSCs and AA-treated Group), 7 rats: Four weeks following diabetes and DR confirmation as in groups II and III, 1x106 of cultured and green fluorescent protein (GFP) labeled AMSCs[15] together with AA were given as in group III.

The rats in group I (control) and its corresponding experimental groups II, III and IV were sacrificed 8 weeks after confirmation of diabetes.

In Vitro Studies

Isolation and propagation of BMHSCs[16] and AMSCs[17] from rats

For BMHSCs isolation, femurs and tibiae of the donor rat were dissected under sterile conditions, then all connective tissue connected to the bones was carefully removed. The BM was obtained by flushing femurs and tibiae with Dulbecco's modified Eagle's medium (DMEM) (GIBCO/BRL), supplemented with 10% fetal bovine serum (FBS) (GIBCO/BRL).

For AMSCs isolation, rat was euthanized with CO_2, and the adipose tissue was extracted from its abdomen. After washing the adipose tissues with saline solution, they were

incubated for 40 minutes at 37 °C in DMEM containing 1% penicillin–streptomycin and 0.2% collagenase mixed solution (GIBCO/BRL). After centrifuging (at 630 g for 10 minutes) the cell suspension, the stromal vascular fraction (SVF) was collected.

A density gradient [Ficoll/Paque (Pharmacia)] was used to isolate mononucleated cells, which were then re-suspended in 1% penicillin-streptomycin culture medium (GIBCO/BRL). Cells were cultured in 5% humidified CO2 incubator for 12- 14 hr at 37° C. When large colonies (80-90% confluence) developed, two PBS washes were performed, and the cells were processed with 0.25% trypsin in 1 ml Ethylene Diamine Tetra Acetate (EDTA) (GIBCO/BRL). Cells were re-suspended with serum-supplemented medium after centrifugation (at 2400 rpm for 20 minutes) and then incubated in 50 cm2 Falcon Culture flasks. On day 14, trypsinized colonies of cells were counted and referred to as 1st-passage cultures.

Characterization of BMHSCs and AMSCs[18]

At the end of the third passage, trypsinized adherent cells were adjusted to 1×10^6 cells/ml using a hemocytometer, then incubated with 10µl monoclonal antibodies: CD34 and CD44 (Beckman coulter, USA) in the dark at 4°C. After 20 minutes, each tube of monoclonal-treated cells received 2 ml of PBS containing 2% fraction crystallizable solution (FCS), then mixture was centrifuged at 2500 rpm for 5 minutes, discarded the supernatant, and re-suspended in 500µl PBS containing 2% FCS. The CYTOMICS FC 500 Flow Cytometer (Beckman Coulter, FL, USA) was used for cell analysis, and CXP Software version 2.2 was used to interpret the results. The immunohistochemical characterization of CD34 and CD44 was performed using streptavidin immunoperoxidase method.

Labeling of BMHSCs with Feridex[19] and AMSCs with GFP[15]

For labeling, BMHSCs were incubated with ferumoxides injectable solution (25µg Fe/ml, Feridex) for 24 hours in culture medium with 375ng/ml polylysine (added 1 hour before incubation). The histological assessment of the labeling was performed with Prussian blue. Feridex-labeled BMHSCs were washed in PBS, trypsinized, and resuspended in 0.01 Mol/L PBS at a concentration of 1x106 cells/ml. During the 4th passage, AMSCs were harvested and labeled with GFP to be examined using a fluorescent microscope.

Animal Studies

Electrophysiological study

Electroretinogram (ERG) was performed, the rats were dark-adapted for at least 2 hours before being prepped in a dim red light. Rats were given an intramuscular injection of ketamine and xylazine, and their pupils were dilated with 0.5% tropicamide/0.5% phenylephrine before being placed on a heating pad. To improve electrical conductivity, hydroxyethyl cellulose was utilized to moisten the cornea and conjunctiva. A gold wire loop electrode on the cornea and a gold wire reference electrode on the sclera were used to record ERGs. Between 0.3 and 1000 Hertz, responses were amplified and bandpass filtered (Hz). A computer-assisted signal averaging technique was used to average the ERGs (Power Lab). For stimulation, a ganzfeld bowl (LACE Electronica) with a xenon source was used. The a- and b-waves' amplitudes were measured[20].

Serological Study

Before sacrifice, blood samples from rats' tail veins were taken at the end of the experiment (8^{th} week after confirmation of diabetes) for estimating blood glucose levels. Then, rats were sacrificed by cervical dislocation under ether anaesthesia[21].

Biochemical Study

The posterior segment of the right eye specimen from each rat of groups I, II, III and IV was separated and homogenized in the deep freezer in 1 ml of normal saline using a homogenizer (Ortoalresa, Spain). Homogenates were centrifuged for 15 minutes at 1000 X g. After collecting the supernatant in Eppendorf tubes, it was stored in the deep freezer at -20°C[22]. Bio-diagnostic colorimetric assay kits (Biodiagnostic, Cairo, Egypt) were used to measure malondialdehyde (MDA)[23], superoxide dismutase (SOD) and tumor necrosis factor alpha TNFα[22] in tissue homogenates.

Histological Study

For 48 hours, the left eye specimens were fixed in 10% formol saline. Paraffin blocks and 5µm thick sections were prepared for the following:

1. Hematoxylin and eosin stain (H&E)[24].
2. Perls Prussian blue stain[25].
3. Immunohistochemical staining using the avidin-biotin peroxidase complex technique[26] for:
    a. Caspase3 (RB-1197-R7, Lab Vision Corporation, USA) immunostaining, the marker for apoptosis.
    b. Proliferating cell nuclear antigen (PCNA) (Clone PC10, Lab Vision Corporation, USA) immunostaining, the marker for progenitor cells.

For 60 minutes, 0.1ml of prediluted (2-4µg/ml) primary rabbit polyclonal Caspase3 antibody was applied to sections. A tonsil specimen was used as the positive tissue control and the positive cells showed cytoplasmic reaction. In addition, 0.1 ml of prediluted (1:50-1:500) primary mouse monoclonal PCNA antibody was applied to sections for 60 minutes. A small intestine specimen was used as the positive tissue control and the positive cells showed nuclear reaction. On the other hand, one of the retina sections was used as the negative tissue control by omitting the primary antibody step.

Morphometric Study

Using Leica Qwin 500 LTD image analysis (Cambridge, UK), the following measurements were performed in 10 high PFs in the control and experimental groups:

1. Thickness of retina and Area (μ2) of dark nuclei & vacuolations of granular cell layer (GCL); using interactive measurements menu.
2. Area% of caspase3 and PCNA positive immunoexpression (IE); using binary mode.

Quantitative polymerase chain reaction (qPCR)

For formalin-fixed paraffin-embedded (FFPE) retina specimens, reverse transcription is carried out with the SuperScript First-Strand Synthesis System for reverse transcriptase (RT)-PCR, based on In*vitro*gen's protocol[27]. The RPE65 and CYP46a1 gene specific primers were retrieved oligonucleotide primers (f: 5'-TGACAAGGTCGACACAGGCAGAAA3') (r: 5'-AAATTCAAAGGCTTGACGAGGCCC3') and (f: 5' -GCGGACCTGAGTCTGAAGAG-3') (r: 5'-AATCACAACTCCGCTTCTGG-3') respectively′. The gene-specific and reverse primer pairs were combined, and the primer concentrations were standardized. The concentration of each primer (forward or reverse) in the mixture is 5 pmol/μl. The ABI Prism standard deviation score (SDS) 7000 was used to run the PCR program. The SDS 7000 software was used to analyze the real-time PCR results. With the following primers (forward primer: 5′-CCTTCCTGGGCATGGAGTCCT-3′ & reverse primer: 5′- GGAGCAATGATCTTGATCTTC-3′), β-actin was used as an internal control to normalize data.

Statistical Analysis[28]

Quantitative data were summarized as means and standard deviations and compared using Analysis of variance (ANOVA) followed by Bonferroni post-hoc test. *P-values* <0.05 were considered statistically significant. Calculations were made on Statistical package of the social sciences (SPSS) version 18.0 for Windows (IBM Corporation, USA).

RESULTS

Lethargy and polyuria were observed in the diabetic group that improved in the treated groups by the end of the experiment. Four diabetic rats died during the experiment, one rat died eight days, two rats died twenty-six days and one rat died thirty-seven days following STZ injection and were compensated.

In Vitro Data

Characterization of BMHSCs and AMSCs

Bone marrow HSCs appeared pleomorphic, immunostaining showed positive brownish membranous reaction for CD34 (Figure 1a) and negative for CD44 (Figure 1b). Immunophenotyping of BMHSCs by flow cytometry showed 98.4 % of cells positive for CD34 (Figure 1c). Adipose MSCs mostly appeared as spindle cells, immunostaining revealed positive brownish membranous reaction for CD44 (Figure 1d) and negative for CD34 (Figure 1e). Immunophenotyping of AMSCs by flow cytometry exhibited 99.1 % of cells positive for CD44 (Figure 1f).

Animal Data

Electrophysiological Results (Figure 2)

The mean amplitude of a wave in ERG was (-1.86±0.13), (-7.61±1.38), (-4.4±1.16) and (-6.3±1.52) in groups I, II, III and IV respectively. In addition, the mean amplitude of b wave in ERG was (74.06±5.1), (37.95±9.54), (60.5±6.86) and (48.9±5.28) in groups I, II, III and IV respectively. The previous data denoted a significant increase (P<0.05) in group I compared to all groups, in group III compared to groups II and IV and in group IV compared to group II.

Serological & Biochemical Results (Table 1)

The mean values of blood glucose indicated a significant increase in group II compared to the other groups. The mean MDA, SOD and TNFα values revealed a significant increase in mean MDA and mean TNFα values, in addition to a significant decrease in mean SOD values in the diabetic group compared to all other groups and in AMSCs group versus control and BMHSCs group.

Histological Results

Haematoxylin and Eosin (H&E) Stained Sections

Group I was subdivided into three subgroups, (IA, IB and IC), the normal histological architecture was observed in all control sections; demonstrating sclera, choroid with choriocapillaries and retina; recruited retinal pigmented epithelium (RPE), photoreceptor layer (PL), outer nuclear layer (ONL), outer plexiform layer (OPL), inner nuclear layer (INL), inner plexiform layer (IPL) and ganglion cell layer (GCL) (Figure 3a). Closer observation showed the sclera exhibiting fibroblasts and collagen bundles, choriocapillaries, pale nuclei of RPE and ONL (Figure 3b). In addition, OPL and IPL revealed interconnected processes, the INL and GCL demonstrated pale nuclei (Figure 3c).

Four weeks following confirmation of diabetes, sections in the retina of a diabetic rat (Group II) showed partial detachment of RPE, some dark nuclei in ONL, INL and GCL, in addition to vacuolations in INL (Figure 3d). After 8 weeks, retinal sections clarified completely detached RPE and capillaries in the INL and GCL (Figure 3e.). Closer observation demonstrated separations in PL, dark nuclei in the ONL and INL, congested capillaries in INL and GCL, in addition to vacuolations in GCL (Figure 3f). Other retinal sections demonstrated some areas of thickening in the IPL, occasional ones contained dispersed nuclei of INL into IPL, while others appeared with disorganized ONL and INL (Figure 3g). Closer observation showed rarefied OPL, separations in INL and vacuolations in INL sometimes extending into IPL (Figure 3h).

Sections of group III revealed choriocapillaries, apparently normal RPE, PL, ONL, OPL, INL, IPL and GCL (Figure 4a). Close observation showed pale nuclei of RPE, minimal separations among PL, few dark nuclei in ONL, minimal rarefactions in OPL, multiple pale and few dark nuclei besides minimal vacuolations in INL (Figure 4b). In addition, few focal rarefactions in IPL were noticed, pale nuclei and minimal vacuolations were seen in GCL (Figure 4c).

Group IV demonstrated choriocapillaries, apparently normal RPE, PL, ONL, OPL, INL, IPL and GCL (Figure 4d). Close observation showed dark nuclei of RPE, minimal separations among PL and ONL, some dark nuclei in ONL and minimal rarefactions in OPL (Figure 4e). In addition, some focal rarefactions in OPL and IPL, some dark nuclei, minimal separations and vacuolations in INL, besides few dark nuclei and few vacuolations in GCL (Figure 4f).

Prussian Blue (Pb)-Stained & GFP-Labeled Sections

Sections in groups I and II showed Pb negative staining in all layers of the retina (Figures 5a,b). Group III demonstrated multiple Pb positive pleomorphic cells in all layers of the retina (Figure 5c). In fluorescent labeled sections, groups I and II showed no GFP labeled cells (Figures 5d,e). While, in group IV multiple labeled cells were detected (Figure 5f).

Immunohistochemical Stained Sections

a. In Caspase3 immunostained sections, group I showed negative IE (Figure 6a). While, in group II extensive positive IE was found among all layers particularly the photoreceptor layer (Figure 6b). On the other hand, group III revealed minimal positive IE among all layers (Figure 6c). In group IV, obvious positive IE was evident among all layers compared to group III (Figure 6d).

b. In PCNA immunostained sections, group II revealed few positive nuclei in the ONL, INL and GCL (Figure 6e). On the other hand, group III recruited multiple positive nuclei in the ONL, INL and GCL (Figure 6f). In group IV, some positive nuclei were evident in the ONL, INL and GCL (Figure 6g).

Morphometric results

Concerning the mean thickness of the retina, it was (148.99±4.58), (227.01±27.31), (159.45±20.78) and (164.96±8.35) in groups I. II, III and IV respectively. A significant increase (P<0.05) was found in group II compared to the other groups. The mean area of dark nuclei of GCL was (879.88±219.35), (226.02±50.8), (371.72±76.67) and that of vacuolations of GCL was (178.79±40.45), (12.58±2.92), (34.53±6.06) in groups II, III and IV respectively, indicating a significant decrease in group III compared to groups II and IV and in group IV compared to group II (Figure 7a). The mean area% of caspase3 +ve IE was (15.64±1.13), (1.60±0.36) , (3.72±0.52) and that of PCNA +ve IE was (1.85±0.44), (5.49±0.37), (3.81±0.49) in groups II, III and IV respectively, denoting a significant decrease and increase respectively in group III compared to groups II and IV and in group IV compared to group II (Figure 7b).

qPCR results

The mean RPE65 and CYP46a1 gene values in ng ± SD were (2.50±0.15) and (1.85±0.20) in group I, (0.90±0.05) and (0.59±0.05) in group II, (2.25±0.08) and (1.66±0.04) in group III, (1.56±0.21) and (1.50±0.13) in group IV respectively. The previous values indicated a significant (P≤0.05) decrease in group II compared to all other groups, in group IV versus control and group III and in group III versus control (Figures 7c,d).

Table 1: Mean values ± standard deviation (SD) of blood glucose, MDA, SOD and TNFα in control and experimental groups

Groups	Blood glucose level mg/dl	MDA nM/mg	SOD U/mg	TNF pg/mg
Group I	96.7 ±6.3	2.03±0.12	8.12±0.34	2.44±0.32
Group II	389.6 ±18.68[a]	7.20±0.25[a]	2.38±0.28[a]	9.05±1.05[a]
Group III	142.3 ±7.61	2.02±0.14	7.78±0.44	2.48±0.09
Group IV	155.8 ±5.12	3.10±0.18[b]	5.80±0.52[b]	3.97±0.31[b]

Significant (P≤ 0.05)

a significant versus other groups.

b significant versus groups I and III.

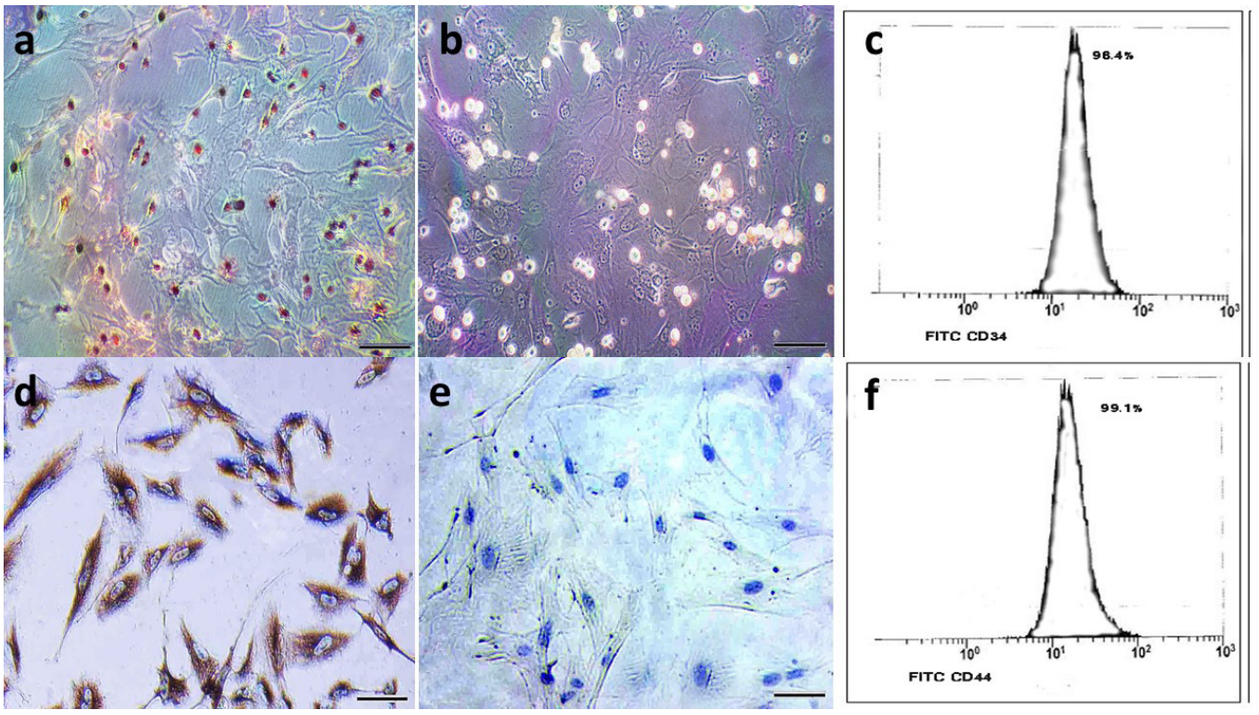

Fig. 1: (a) CD34 positive pleomorphic cells. (b) CD44 negative immunoreactivity (Phase contrast microscopy x 100). (c) Immunophenotyping of BMHSCs 98.4 % are positive for CD34 (Flow Cytometry). (d) CD44 positive spindle cells (e) CD34 negative immunoreactivity (Phase contrast microscopy x 100). (f) Immunophenotyping of AMSCs 99.1 % are positive for CD44 (Flow Cytometry).

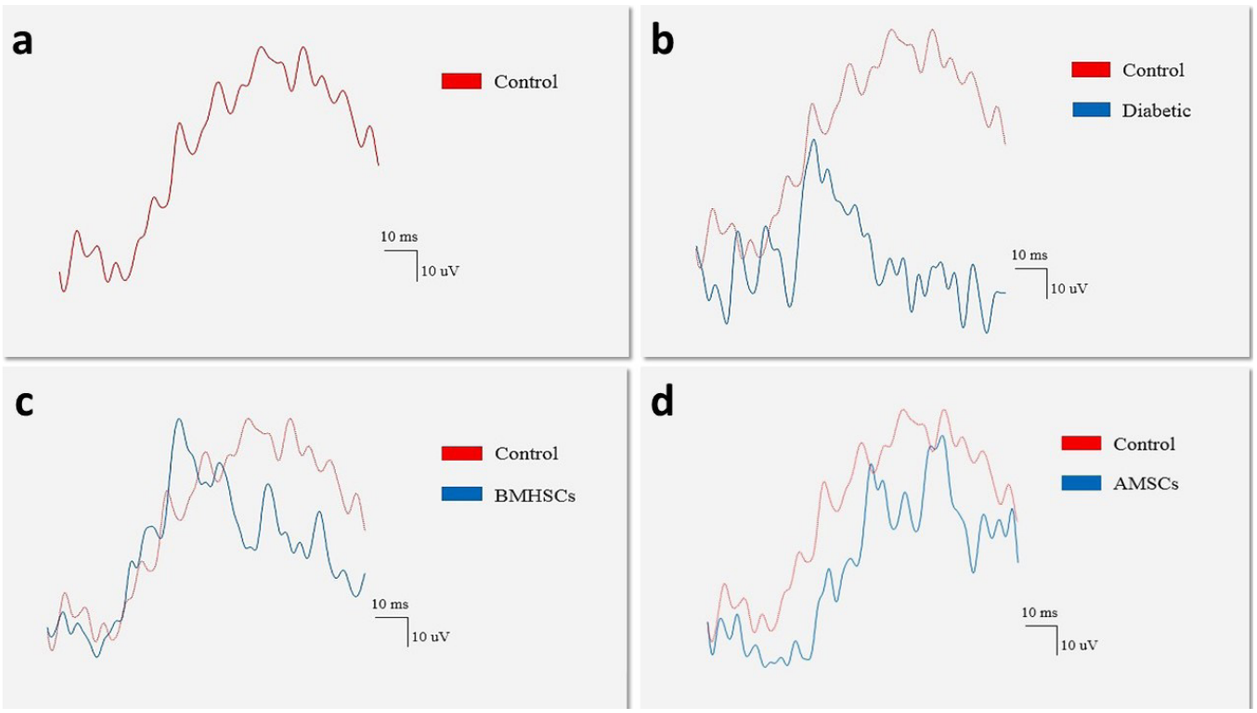

Fig. 2: (a) ERG of group I. (b) ERG of groups II (blue) and I (red). (c) ERG of groups III (blue) and I (red). (d) ERG of groups IV (blue) and I (red).

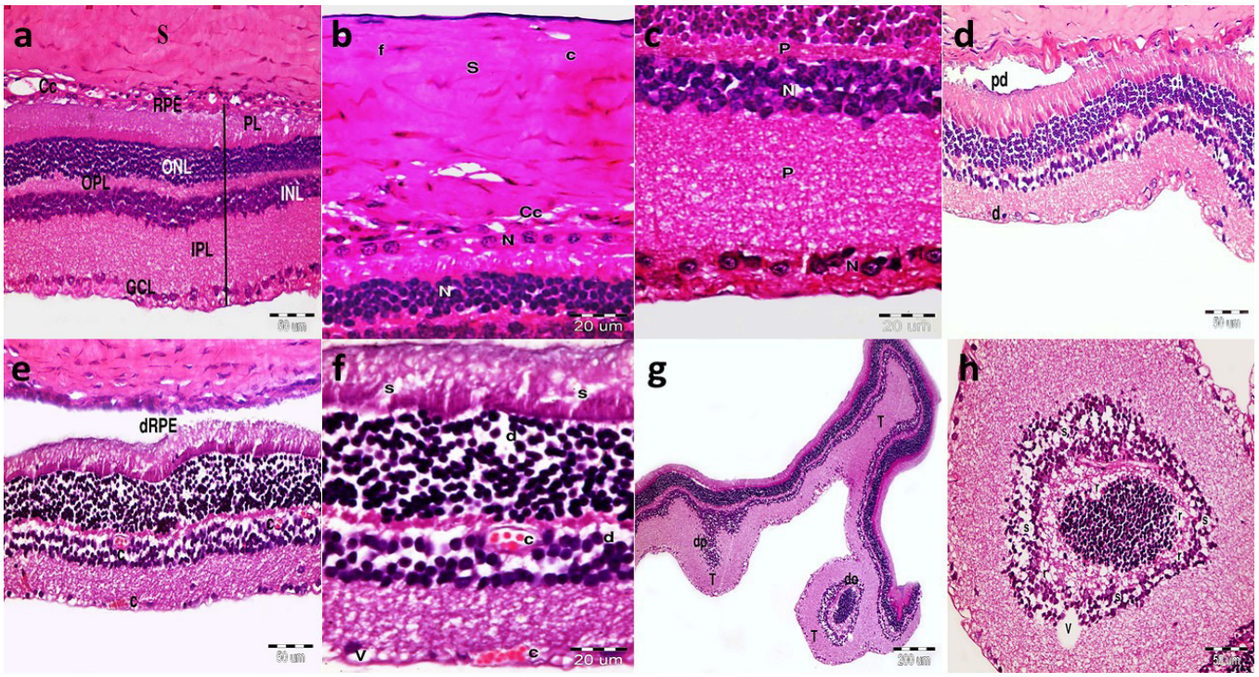

Fig. 3: H&E stained sections: Group I shows (a) Sclera (S), choriocapillaris (Cc) and retina (black line) with RPE, PL, ONL, OPL, INL, IPL and GCL (x400). (b) Sclera (S), fibroblasts (f), collagen bundles (c), choriocapillaries (Cc), pale nuclei (N) of RPE and ONL (x1000) (c) OPL and IPL recruiting interconnected processes (P), INL and GCL pale nuclei (N) (x1000). Group II shows (d) 4 weeks after diabetes confirmation, partial detachment (pd), some dark (d) nuclei in ONL, INL, GCL and vacuolations (v) in INL (x400). (e) 8 weeks after diabetes confirmation, detached RPE (dRPE), capillaries (c) in the INL and GCL (x400). (f) Separations (s) in PL, dark nuclei (d) in the ONL and INL, congested capillaries (c) in INL and GCL, vacuolations (V) in GCL (x1000). (g) Areas of thickening (T) in the IPL, one contains dispersed nuclei (dp) of INL into IPL, another with disorganized (do) ONL and INL (x100). (h) rarefied (r) OPL, separations (s) in INL and vacuolations in INL extending into IPL (V) (x400).

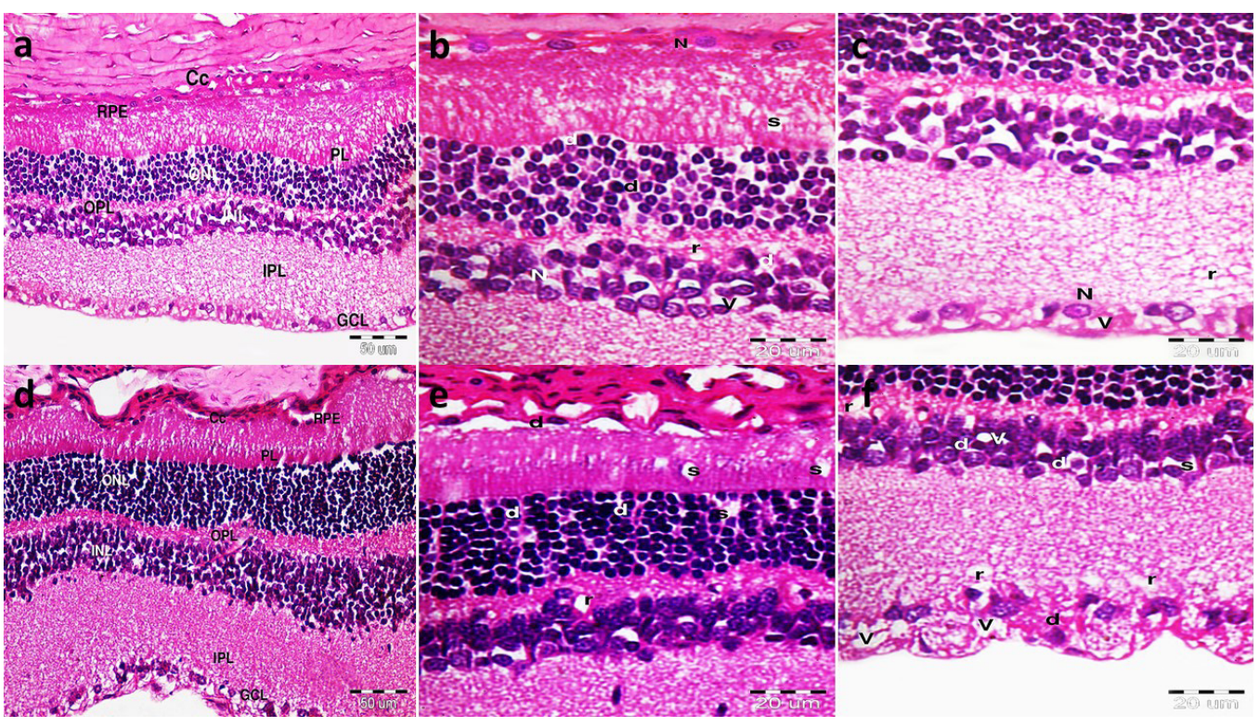

Fig. 4: H&E stained sections: Group III shows (a) Choriocapillaries (Cc), apparently normal RPE, PL, ONL, OPL, INL, IPL and GCL (x400). (b) Pale nuclei (N) of RPE, minimal separations (s) among PL, few dark (d) nuclei in ONL, minimal rarefactions (r) in OPL, multiple pale nuclei (N), few dark (d) nuclei and minimal vacuolations (V) in INL (x1000). (c) Few focal rarefactions (r) in IPL, pale nuclei (N) and minimal vacuolations (V) in GCL (x1000). Group IV shows (d) Choriocapillaries (Cc), apparently normal RPE, PL, ONL, OPL, INL, IPL and GCL (x400). (e) Dark nuclei (d) of RPE, minimal separations (s) among PL and ONL, some dark nuclei in ONL and minimal rarefactions (r) in OPL (x1000). (f) Some focal rarefactions (r) in OPL and IPL, some dark nuclei (d), minimal separations (s), vacuolations (V) in INL and few dark nuclei (d) and few vacuolations (V) in GCL (x1000).

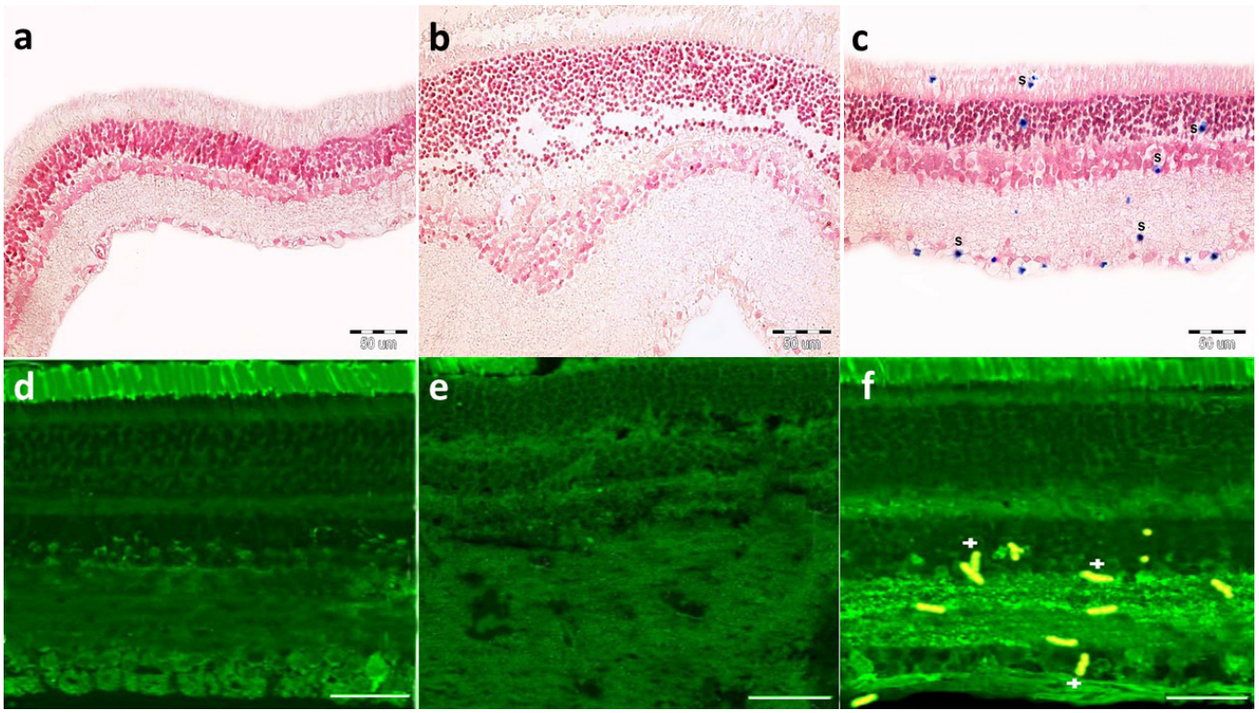

Fig. 5: (a) Negative staining in group I. (b) Negative staining in group II. (c) Multiple +ve pleomorphic cells among all layers in group III (Prussian blue, x400). (d) No fluorescent labeled cells in group I. (e) No fluorescent labeled cells in group II. (f) Multiple labeled cells in group IV (GFP, x 400).

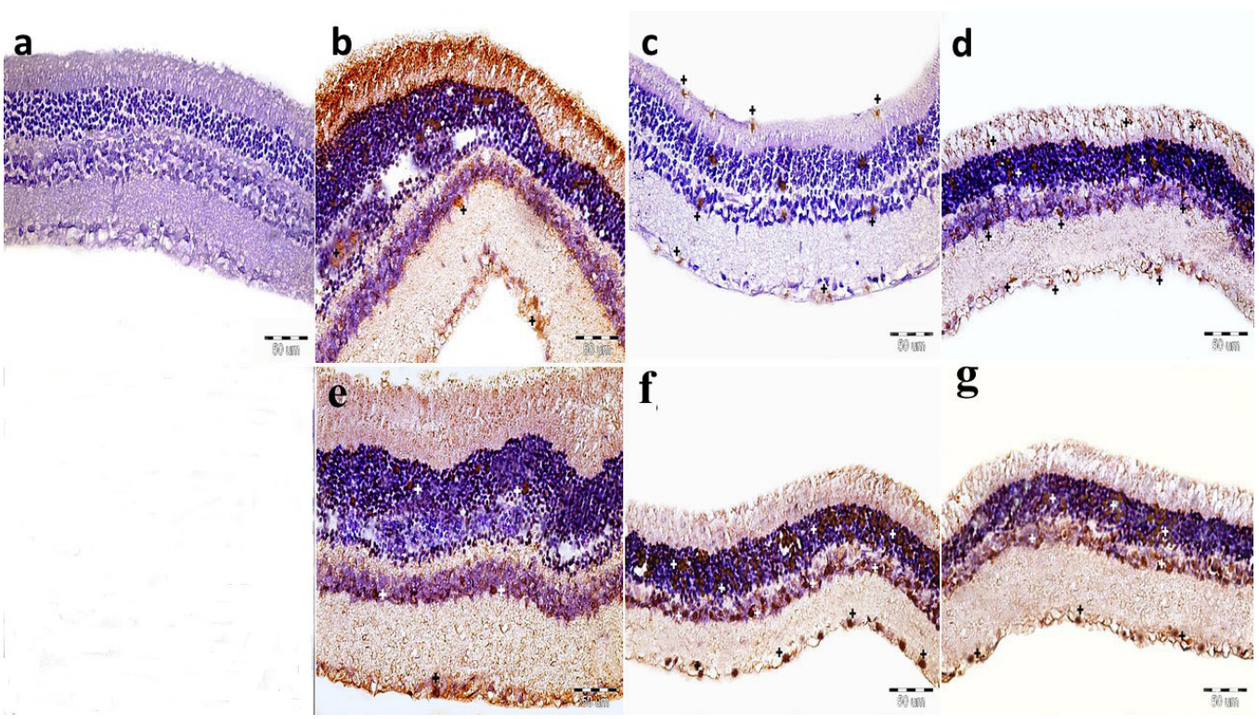

Fig. 6: (a) Negative IE in group I. (b) Extensive positive IE (white and black +) among all layers particularly the photoreceptor layer in group II. (c) Minimal positive IE (white and black +) among all layers in group III. (d) Obvious positive IE among all layers (white and black +) in group IV (Caspase3 immunostaining, x 400). (e) Few positive nuclei (+) in the ONL, INL and GCL in group II. (f) Multiple positive nuclei (+) in the ONL, INL and GCL in group III. (g) Some positive nuclei (+) in the ONL, INL and GCL in group IV (PCNA immunostaining, x 400).

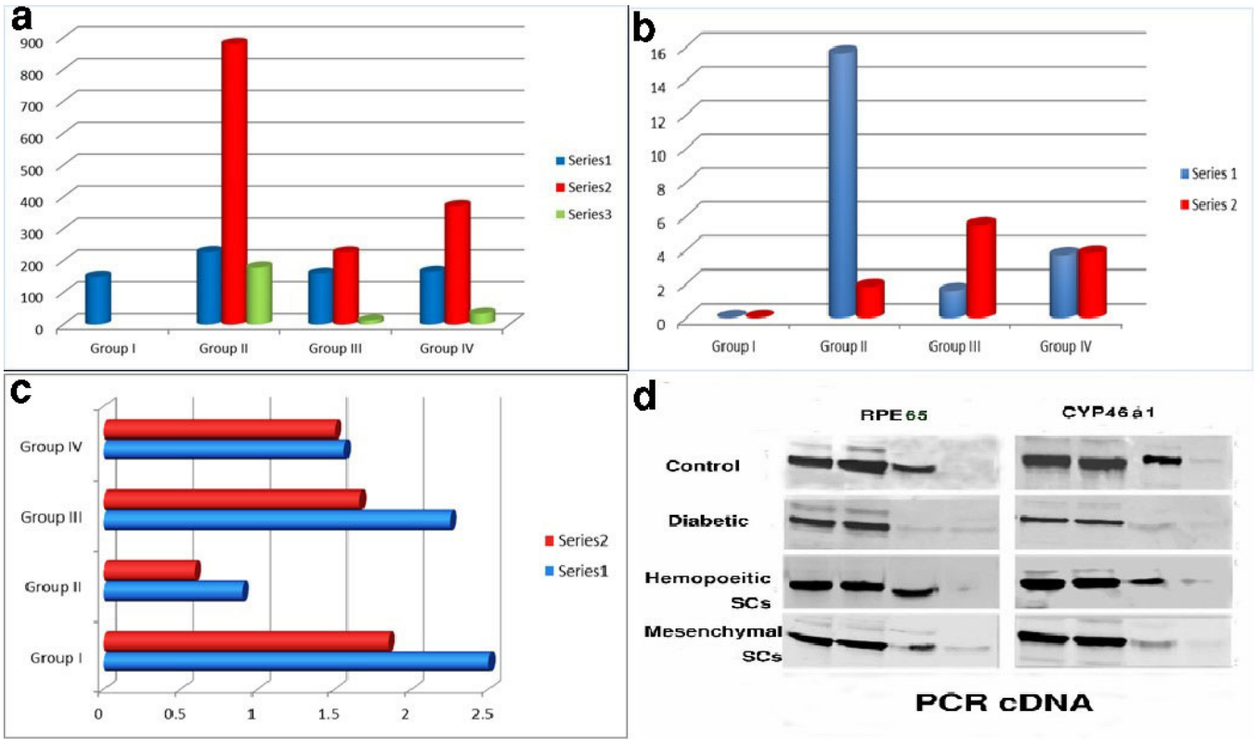

Fig. 7: Histograms of (a) Mean thickness of the retina, dark nuclei and vacuolations of GCL (b) Mean area% of caspase3 IE and PCNA IE (c) Mean qPCR of RPE65 and CYP46a1 gene values in groups I, II, III and IV (d) cDNA of RPE65 and CYP46a1 genes in groups I, II, III and IV.

DISCUSSION

The present study aimed at investigating and comparing the enhanced therapeutic effect of BMHSCs versus AMSCs by AA on STZ induced early DR in male albino rat model. STZ was used for induction of type I diabetes. The expected duration of development of DR was 4 weeks following STZ injection. This was supported by ERG examination performed by Rong *et al*.[12].

In the treated groups (III and IV), AA was administered concomitantly with SCs . AA is known for its anti-inflammatory and antioxidant properties; it is capable of scavenging ROS and reducing pro-inflammatory cytokines. Recent research suggests the benefits of AA for promoting stem cell renewal and maintaining stemness[29].

The mean ERG values of amplitude of a and b waves denoted a significant increase in group III compared to groups II and IV and in group IV compared to group II. The previous results indicated deterioration of neuronal transmission in diabetic rats that appeared to improve in the treated groups. Changes in ERG may attribute to neuronal malfunction, changes in neurotransmitter levels and cell death in neural retina. Furthermore, increased vascular permeability in diabetic rodents that occurs as early as one week following hyperglycemia may influence neuronal function due to neurovascular coupling[30]. It was reported that SCs can integrate into the inner retina and differentiate into retinal glial cells; also, SCs secrete a number of proteins known as neurotrophic factors, which are linked to a slowed degeneration process in the retina. Consequently, improved ERG response was recorded in treated groups[31].

A significant increase was reported in the mean blood glucose values in diabetic group and a significant decrease was reported in SCs treated groups. Zickri *et al*[18] suggested that the hyperglycemic lowering effect may be related to that SCs improve diabetic glycemic control. The mean MDA, SOD and TNFα values indicated a significant increase in MDA and TNFα, in addition to a significant decrease in SOD in group II compared to all other groups and in group IV versus group III. The previous findings denoted oxidative stress and inflammation that progressed to degeneration in diabetic group and regressed in treated groups.

SCs could improve antioxidative capacity by upregulating certain proteins which ameliorate oxidative stress and others that regulate the expression of genes related to anti-inflammatory and antioxidant defense. In addition to promotion of SOD2 protein expressions and suppression of MDA levels, the immunomodulation property of SCs enable them to attenuate the inflammatory response directly through inhibition of the pro-inflammatory cytokines including TNF- α[32].

In the present study, group II demonstrated some areas of thickening in the IPL. The previous results were confirmed by a significant increase in the mean thickness of the retina in group II compared to the other groups. Going with, Yun[33] referred thickening to be due to vascular leakage into retinal tissue. It was confirmed that increased

TNF-α in early stages of DR is involved in pericytes' loss by inducing apoptosis thus reducing tight junction.

Detached RPE, dispersed nuclei of INL into IPL and disorganized ONL and INL with dark nuclei, and vacuolated areas in disorganized IPL, in addition to vacuolations in GCL, separations in PL and INL, rarefied OPL and congested capillaries were seen in the INL and GCL of diabetic rats, indicating degenerative changes of the retina. Liu and Wu[34] stated that hyperglycemia can damage the BRB, blood leakage from central retinal artery triggers ischemia in surrounding retina. Consequent neovascularization in the form of abnormal growth of new vessels as an attempt to increase oxygen supply to counteract hypoxia, in addition to structural disorganization and cellular loss will develop.

Group III revealed pale nuclei of RPE, few dark nuclei in ONL and INL, minimal vacuolations in INL and GCL, minimal separations among PL, in addition to minimal focal rarefactions in OPL and IPL. While, group IV showed some dark nuclei of RPE, ONL, INL and few dark nuclei in GCL, minimal vacuolations in INL and few vacuolations in GCL, minimal separations among PL, ONL and INL, in addition to minimal rarefactions in OPL and IPL. The previous findings indicated amelioration of degenerative changes and were confirmed by a significant decrease in the mean area of dark nuclei and that of vacuolations of GCL that was found in group III compared to groups II and IV, also in group IV compared to group II.

Neurotrophic factors secreted by SCs bind to their receptors on recipient cells to enhance neural cell survival, differentiation, axonal growth and attachment, as well as preventing retinal degeneration, improving retinal morphology and function. Intravitreal administration of murine SCs decreased oxidative stress in retina and prevented ganglion cell loss. In addition, injected cells differentiated into pericytes in *vivo*, preserving BRB integrity and differentiating into indispensable cells such as photoreceptor cells in DR models[35].

In group II extensive positive caspase3 IE was found among all layers particularly the PL. On the other hand, group III revealed minimal positive IE among all layers particularly the PL. In group IV, obvious positive IE was evident among all layers compared to group III. These observations proved apoptosis in the diabetic group that improved in treated groups. They were confirmed by a significant decrease in the mean area % of caspase3 positive IE in group III compared to groups II and IV and in group IV compared to group II.

In agreement, in DR caspase-3 expression showed a significant rise, and this was explained that, increased levels of oxidative stress and apoptosis in DR have been linked to mitochondrial dysfunction. The latter affects both retinal neurons and vascular cells by a vicious cycle, activates inflammatory mediators and ROS production, which damages DNA, and eventually leads to apoptotic cell death[36].

In support, it was proved that SCs can effectively delay the photoreceptor and glial cells apoptosis, promote neuroprotection and neurogenesis. SCs are thought to exert their regeneration and repair effects by "empowering" cells rather than simply replacing them. SCs create a favorable environment for tissue regeneration by inhibiting local inflammation and immunological responses (immunomodulation)[37].

Group II revealed few positive PCNA IE in nuclei of the ONL, INL and GCL. On the other hand, group III recruited multiple positive nuclei, while in group IV some positive nuclei were evident in the ONL, INL and GCL. A significant increase in mean area % of PCNA positive IE was confirmative in group III compared to groups II and IV, in group IV compared to group II. In retina, SCs can generate multipotential progenitors, which were shown to have upregulated PCNA markedly affected by DM, which is an intranuclear polypeptide, expressed only in proliferating cells and used as an indicator of the proliferation activity[38].

The mean RPE65 and CYP46a1 gene values indicated a significant decrease in group II compared to all other groups, in group IV versus control and group III and in group III versus control. Zhang *et al*[37] confirmed that inhibition of RPE65 and CYP46a1 in retinal degeneration impairs retinal function. Moreover, bioactive exchanges, including proteins and nucleic acids are transported from SCs to stressed cells. As a result, angiogenesis is promoted, and cell survival and/or renewal in injured tissues is improved[39].

In the present study, ERG, biochemical, histological, immunohistochemical and PCR findings proved more obvious and detectable amelioration of morphological and quantitative confirmative results in response to BMHSCs versus AMSCs therapy in DR. Umbilical cord MSCs when transplanted into diabetic rats, showed attenuation in retinal vascular dysfunction. While, HSCs have been shown to exert a repairing effect on microvascular endothelial cells and pericytes in the retina, as well as inhibiting pathological neovascularization[40].

Group III demonstrated multiple Pb +ve pleomorphic cells in all layers of the retina. While, in group IV multiple labeled cells were detected. In accordance, Abdel Halim *et al*[19] who described the use of Pb staining to visualize the iron particles in Feridex labeled SCs. Likewise, Tang *et al*[15] reported the use of GFP labeled MSCs and viewed them under fluorescence microscope. The authors added that GFP is a cell marker that cannot be found in living organisms, so it is an indication that the cell was administered externally and is not part of the organism.

Diabetes type I induced degenerative changes indicating the development of early DR that progressed without treatment. BMHSCs and AMCs therapy proved to reverse the degenerative changes. AA enhanced regenerative effect of BMHSCs was more obvious, indicating that it could be used as a therapeutic modality for treating DR. The

enhanced therapeutic effect was confirmed and compared by electrophysiological, histological, morphometric, biochemical and serological studies.

ACKNOWLEDGMENTS

Dr. Hala Gabr, Professor of clinical pathology, Faculty of Medicine, Cairo University, Egypt performed serological and biochemical procedures. Mr. Kareem Hassan, a technician at the Medical Histology and Cell Biology Department, assisted in preparation of specimens.

CONFLICT OF INTERESTS

There are no conflicts of interest.

REFERENCES

1. Spencer BG, Estevez JJ, Liu E, Craig JE, Finnie JW. Pericytes, inflammation, and diabetic retinopathy. Inflammopharmacology. 2020; 28(3): 697-709. DOI: 10.1007/s10787-019-00647-9
2. Vujosevic S, Aldington SJ, Silva P, Hernández C, Scanlon P, Peto T, Simó R. Screening for diabetic retinopathy: new perspectives and challenges. Lancet Diabetes Endocrinol. 2020; 8(4): 337-347. doi: 10.1016/S2213-8587(19)30411-5.
3. Bandello F, Toni D, Porta M, Varano M. Diabetic retinopathy, diabetic macular edema, and cardiovascular risk: the importance of a long-term perspective and a multidisciplinary approach to optimal intravitreal therapy. Acta Diabetol. 2020; 57(5): 513-526. doi: 10.1007/s00592-019-01453-z.
4. Maalej A, Khallouli A, Choura R, Ben Sassi R, Rannen R, Gharsallah H. The effects of hyperbaric oxygen therapy on diabetic retinopathy: A preliminary study. J Fr Ophtalmol. 2020; 43(2): 133-138. doi: 10.1016/j.jfo.2019.07.005.
5. Vinci MC, Gambini E, Bassetti B, Genovese S, Pompilio G. When Good Guys Turn Bad: Bone Marrow's and Hematopoietic Stem Cells' Role in the Pathobiology of Diabetic Complications. Int J Mol Sci. 2020; 21(11): 3864. doi: 10.3390/ijms21113864.
6. Jalilian E, Elkin K, Shin SR. Novel Cell-Based and Tissue Engineering Approaches for Induction of Angiogenesis as an Alternative Therapy for Diabetic Retinopathy. Int J Mol Sci. 2020; 21(10): 3496. doi: 10.3390/ijms21103496.
7. Saadane A, Mast N, Trichonas G, Chakraborty D, Hammer S, Busik JV, Grant MB, Pikuleva IA. Retinal Vascular Abnormalities and Microglia Activation in Mice with Deficiency in Cytochrome P450 46A1-Mediated Cholesterol Removal. Am J Pathol. 2019; 189(2): 405-425. doi: 10.1016/j.ajpath.2018.10.013.
8. Miao A, Lu J, Wang Y, Mao S, Cui Y, Pan J, Li L, Luo Y. Identification of the aberrantly methylated differentially expressed genes in proliferative diabetic retinopathy. Exp Eye Res. 2020; 199: 108141. doi: 10.1016/j.exer.2020.108141.
9. Caritá AC, Fonseca-Santos B, Shultz JD, Michniak-Kohn B, Chorilli M, Leonardi GR. Vitamin C: One compound, several uses. Advances for delivery, efficiency and stability. Nanomedicine. 2020; 24: 102117. doi: 10.1016/j.nano.2019.102117.
10. Karimi SA, Salehi I, Taheri M, Faraji N, Komaki A. Effects of Regular Exercise on Diabetes-Induced Memory Deficits and Biochemical Parameters in Male Rats. J Mol Neurosci. 2021; 71(5): 1023-1030. doi: 10.1007/s12031-020-01724-3
11. Kamble SP, Ghadyale VA, Patil RS, Haldavnekar VS, Arvindekar AU. Inhibition of GLUT2 transporter by geraniol from Cymbopogon martinii: a novel treatment for diabetes mellitus in streptozotocin-induced diabetic rats. J Pharm Pharmacol. 2020; 72(2): 294-304. doi: 10.1111/jphp.13194.
12. Rong L, Gu X, Xie J, Zeng Y, Li Q, Chen S, Zou T, Xue L, Xu H, Yin ZQ. Bone Marrow CD133+ Stem Cells Ameliorate Visual Dysfunction in Streptozotocin-induced Diabetic Mice with Early Diabetic Retinopathy. Cell Transplant. 2018; 27(6): 916-936. doi: 10.1177/0963689718759463.
13. Zickri MB, Fadl SG, Metwally HG. Comparative Study between Intravenous and Intraperitoneal Stem Cell Therapy in Amiodarone Induced Lung Injury in Rat. Int J Stem Cells. 2014; 7(1): 1-11. doi: 10.15283/ijsc.2014.7.1.1.
14. Picklo MJ, Thyfault JP. Vitamin E and vitamin C do not reduce insulin sensitivity but inhibit mitochondrial protein expression in exercising obese rats. Appl Physiol Nutr Metab. 2015; 40(4): 343-52. doi: 10.1139/apnm-2014-0302.
15. Tang X, Chen F, Lin Q, You Y, Ke J, Zhao S. Bone marrow mesenchymal stem cells repair the hippocampal neurons and increase the expression of IGF-1 after cardiac arrest in rats. Exp Ther Med. 2017; 14(5): 4312-4320. doi: 10.3892/etm.2017.5059.
16. Duman DG, Zibandeh N, Ugurlu MU, Celikel C, Akkoc T, Banzragch M, Genc D, Ozdogan O, Akkoc T. Mesenchymal stem cells suppress hepatic fibrosis accompanied by expanded intrahepatic natural killer cells in rat fibrosis model. Mol Biol Rep. 2019; 46(3): 2997-3008. doi: 10.1007/s11033-019-04736-4.
17. Rezapour-Lactoee A, Yeganeh H, Gharibi R, Milan PB. Enhanced healing of a full-thickness wound by a thermoresponsive dressing utilized for simultaneous transfer and protection of adipose-derived mesenchymal stem cells sheet. J Mater Sci Mater Med. 2020; 31(11): 101. doi: 10.1007/s10856-020-06433-2.
18. Zickri MB, Aboul-Fotouh GI, Omar AI, El-Shafei AA, Reda AM. Effect of Stem Cells and Gene Transfected Stem Cells Therapy on the Pancreas of Experimentally Induced Type 1 Diabetes. Int J Stem Cells. 2018; 11(2): 205-215. doi: 10.15283/ijsc18002.

19. Abdel Halim AS, Ahmed HH, Aglan HA, Abdel Hamid FF, Mohamed MR. Role of bone marrow-derived mesenchymal stem cells in alleviating pulmonary epithelium damage and extracellular matrix remodeling in a rat model of lung fibrosis induced by amiodarone. Biotech Histochem. 2021; 96(6): 418-430. doi: 10.1080/10520295.2020.1814966.

20. Suzumura A, Kaneko H, Funahashi Y, Takayama K, Nagaya M, Ito S, Okuno T, Hirakata T, Nonobe N, Kataoka K, Shimizu H, Namba R, Yamada K, Ye F, Ozawa Y, Yokomizo T, Terasaki H. n-3 Fatty Acid and Its Metabolite 18-HEPE Ameliorate Retinal Neuronal Cell Dysfunction by Enhancing Müller BDNF in Diabetic Retinopathy. Diabetes. 2020; 69(4): 724-735. doi: 10.2337/db19-0550.

21. Yaşar M, Çakmak H, Dündar S, Örenay Boyacıoğlu S, Çalışkan M, Ergin K. The role of microRNAs in corneal neovascularization and its relation to VEGF. Cutan Ocul Toxicol. 2020; 39(4): 341-347. doi: 10.1080/15569527.2020.1813749

22. He M, Long P, Yan W, Chen T, Guo L, Zhang Z, Wang S. ALDH2 attenuates early-stage STZ-induced aged diabetic rats retinas damage via Sirt1/Nrf2 pathway. Life Sci. 2018; 215: 227-235. doi: 10.1016/j.lfs.2018.10.019.

23. Anreddy RNR. Copper oxide nanoparticles induces oxidative stress and liver toxicity in rats following oral exposure. Toxicol Rep. 2018; 5: 903-904. doi: 10.1016/j.toxrep.2018.08.022.

24. Kiernan JA. Histological and histochemical methods: Theory and practice. 5th edition. Arnold publisher, London, New York & New Delhi; 2015: 132-212.

25. Doroudian M, O'Neill A, O'Reilly C, Tynan A, Mawhinney L, McElroy A, Webster SS, MacLoughlin R, Volkov Y, E Armstrong M, A O'Toole G, Prina-Mello A, C Donnelly S. Aerosolized drug-loaded nanoparticles targeting migration inhibitory factors inhibit Pseudomonas aeruginosa-induced inflammation and biofilm formation. Nanomedicine (Lond). 2020; 15(30): 2933-2953. doi: 10.2217/nnm-2020-0344.

26. Suvarna SK, Layton C and Bancroft JD. Immunohistochemical and immunofluorescent techniques. In: Bancroft's Theory and practice of histological techniques, chapter 19, 8th edition. Elsevier, China; 2019: 337-394.

27. Xin-Zhao Wang C, Zhang K, Aredo B, Lu H, Ufret-Vincenty RL. Novel method for the rapid isolation of RPE cells specifically for RNA extraction and analysis. Exp Eye Res. 2012 Sep; 102: 1-9. doi: 10.1016/j.exer.2012.06.003

28. Emsley R, Dunn G, White I. Mediation and moderation of treatment effects in randomized controlled trials of complex interventions. Stat Methods Med Res. 2010; 19(3): 237-270. doi: 10.1177/0962280209105014.

29. Shi Z, Wang Q, Jiang D. Ascorbic acid mitigates the deleterious effects of nicotine on tendon stem cells. Connect Tissue Res. 2021; 62(2): 183-193. doi: 10.1080/03008207.2019.1663349

30. Chesler K, Motz C, Vo H, Douglass A, Allen RS, Feola AJ, Pardue MT. Initiation of L-DOPA Treatment After Detection of Diabetes-Induced Retinal Dysfunction Reverses Retinopathy and Provides Neuroprotection in Rats. Transl Vis Sci Technol. 2021; 10(4): 8. doi: 10.1167/tvst.10.4.8

31. Usategui-Martin R, Fernandez-Bueno I. Neuroprotective therapy for retinal neurodegenerative diseases by stem cell secretome. Neural Regen Res. 2021; 16(1): 117-118. doi: 10.4103/1673-5374.283498.

32. Chen Y, Zhang F, Wang D, Li L, Si H, Wang C, Liu J, Chen Y, Cheng J, Lu Y. Mesenchymal Stem Cells Attenuate Diabetic Lung Fibrosis via Adjusting Sirt3-Mediated Stress Responses in Rats. Oxid Med Cell Longev. 2020; 2020: 8076105. doi: 10.1155/2020/8076105.

33. Yun JH. Hepatocyte growth factor prevents pericyte loss in diabetic retinopathy. Microvasc Res. 2021; 133: 104103. doi: 10.1016/j.mvr.2020.104103.

34. Liu Y, Wu N. Progress of Nanotechnology in Diabetic Retinopathy Treatment. Int J Nanomedicine. 2021; 16: 1391-1403. doi: 10.2147/IJN.S294807.

35. Adak S, Magdalene D, Deshmukh S, Das D, Jaganathan BG. A Review on Mesenchymal Stem Cells for Treatment of Retinal Diseases. Stem Cell Rev Rep. 2021; 17(4): 1154-1173. doi: 10.1007/s12015-020-10090-x.

36. Daniel A, Premilovac D, Foa L, Feng Z, Shah K, Zhang Q, Woolley KL, Bye N, Smith JA, Gueven N. Novel Short-Chain Quinones to Treat Vision Loss in a Rat Model of Diabetic Retinopathy. Int J Mol Sci. 2021; 22(3): 1016. doi: 10.3390/ijms22031016.

37. Zhang Z, Mugisha A, Fransisca S, Liu Q, Xie P, Hu Z. Emerging Role of Exosomes in Retinal Diseases. Front Cell Dev Biol. 2021; 9: 643680. doi: 10.3389/fcell.2021.643680.

38. 38. Qiu X, Wang H, Wang Z, Fu Y, Yin J. Expression of PCNA, Ki-67 and COX-2 in breast cancer based on DCE-MRI image information. J Infect Public Health. 2020; 13(12): 2032-2037. doi: 10.1016/j.jiph.2019.06.024.

39. Najar M, Martel-Pelletier J, Pelletier JP, Fahmi H. Mesenchymal Stromal Cell Immunology for Efficient and Safe Treatment of Osteoarthritis. Front Cell Dev Biol. 2020; 8: 567813. doi: 10.3389/fcell.2020.567813

40. Li XJ, Li CY, Bai D, Leng Y. Insights into stem cell therapy for diabetic retinopathy: a bibliometric and visual analysis. Neural Regen Res. 2021; 16(1): 172-178. doi: 10.4103/1673-5374.286974

الملخص العربى

التأثير العلاجي المحتمل المعزز لحمض الأسكوربيك للخلايا الجذعية المكونة للدم والخلايا الجذعية الوسيطة على الفئران المصابة باعتلال الشبكية السكري المبكر: دراسة هيستولوجية فسيولوجية كيميائية مقارنة

اسماء احمد الشافعي[١]، مها بليغ زكري[١،٢]، سحر محمود منصور[٣]، مروة ابراهيم عبد العزيز[٣]، حسام الدين سيد كريم[٤]، مي عبد العزيز جودة[٥]، دعاء مبروك خالد[٦]

[١]قسم الهيستولوجيا الطبية وبيولوجية الخلية، كلية الطب، جامعة القاهرة، مصر

[٢]كلية طب الفم والأسنان، جامعة المستقبل، مصر

[٣]قسم الهيستولوجيا، معهد بحوث امراض العيون

[٤]قسم علوم الرؤية، وحدة البصريات الفسيولوجية، معهد بحوث امراض العيون، القاهرة، مصر

[٥]قسم الكيمياء الحيوية الطبية والبيولوجيا الجزيئية، كلية الطب، جامعة القاهرة، جامعة بدر، القاهرة، مصر

[٦]قسم الهيستولوجيا وعلم الخلية، كلية الطب، جامعة حلوان، مصر

الخلفية والأهداف: اعتلال الشبكية السكري هو اختلاط خطير للعين لمرض السكري والسبب الرئيسي للعمى وفقدان البصر في كل من البلدان المتقدمة والنامية . هدفت الدراسة الحالية إلى دراسة ومقارنة التأثير العلاجي المحتمل المعزز لحمض الأسكوربيك (AA) للخلايا الجذعية المكونة للدم لنخاع العظم (BMHSCs) إلى الخلايا الجذعية اللحمية الدهنية (AMSCs) على اعتلال الشبكية السكري المبكر الناجم عن الستربتوزوتوسين في ذكر نموذج الجرذ الابيض
الطريقة والنتائج: تم تقسيم ٣٠ ذكر جرذ ابيض بالغ إلى: مجموعة متبرعة: ٢ جرذان, الخلايا الجذعية المكونة للدم لنخاع العظام و الخلايا الجذعية الوسيطة للأنسجة الدهنية ، مزرعة ، التنميط الظاهري والتعريف. المجموعة I (المجموعة الضابطة): ٦ فئران ، المجموعة الثانية (مجموعة اعتلال الشبكية السكري): ٨ فئران ، ٥٠ مجم من الستربتوزوتوسين تم حقنها داخل التجويف البريتوني ، تم تأكيد مرض السكري بعد ٣ أيام من حقن الستربتوزوتوسين من خلال مراقبة مستويات الجلوكوز في الدم. إذا كان مستوى الجلوكوز في الدم لدى الحيوانات اكثر من ٢٠٠ ملغ / ديسيلتر ، فقد تم اعتبارهم مرضى السكري . المجموعة الثالثة (مجموعة اعتلال الشبكة السكري المعالجة ب الخلايا الجذعية المكونة للدم لنخاع العظام وحمض الأسكوربيك): ٧ فئران ، تم حقن ١x١٠٦ من الخلايا الجذعية المكونة للدم لنخاع العظام في التجويف البريتوني حنبا الي جنب مع الإعطاء الفموي لحمض الأسكوربيك بجرعة ٥٠٠ مجم / كجم يوميًا . المجموعة الرابعة (مجموعة اعتلال الشبكة السكري المعالجة ب الخلايا الجذعية الوسيطة المأخوذة من الانسجة الدهنية وحمض الأسكوربيك): تم حقن ٧ فئران ١x١٠٦ من الخلايا الجذعية الوسيطة المأخوذة من الانسجة الدهنية جنبًا إلى جنب مع حمض الأسكوربيك كما في المجموعة الثالثة بعد التاكد من مرض السكري. تم التضحية بالمجموعات الأولى والثانية والثالثة والرابعة ٨ أسابيع بعد التأكد من مرض السكري. تم إجراء دراسات مخطط كهربية الشبكية ، مصلية ، كيميائية حيوية ، نسيجية ،نسيجية كيميائية ، مورفومترية ، كما تم عمل تحليل احصائي. في المجموعة الثانية ، تم العثور على التغيرات العصبية في شبكية العين والتي تراجعت في المجموعتين الثالثة والرابعة. كانت نتائج مخطط كهربية الشبكية وجلوكوز الدم و المالون دايالدهايد و ديسموتاز سوبر أكسيد و TNFالفا و تفاعل البلمرة الكمي مؤكدة.
الاستنتاجات: كان التأثير التجديدي المعزز لحمض الاسكوربيك للخلايا الجذعية المكونة للدم لنخاع العظام أكثر وضوحًا ، مما يشير إلى إمكانية تطبيقه كطريقة علاجية لاعتلال الشبكية